

Heat and mass transfer processes at the most heat-stressed areas of the surface of the descent module

Oleg A. Pashkov* and Boris A. Garibyan^a

Moscow Aviation Institute (National Research University), Moscow, Russia

(Received June 17, 2022, Revised July 21, 2022, Accepted November 7, 2022)

Abstract. The study presents the results of the research of heat and heat exchange processes on the heat-stressed elements of the structure of an advanced TsAGI descent vehicle. The studies were carried out using a mathematical model based on solving discrete analogs of continuum mechanics equations. Conclusions were drawn about the correctness of the model and the dependence of the intensity of heat and mass transfer processes on the most heat-stressed sections of the apparatus surface on its geometry and the catalytic activity of the surface.

Keywords: descent aircraft; gas dynamics; heat and mass transfer; mathematical modeling; multicomponent flow

1. Introduction

One of the most important tasks in designing a descent vehicle, the results of which largely determine its flight performance, is the task of determining the parameters of heat exchange on its surface. In this case, the thermal design of the vehicle usually contradicts the requirements of aerodynamic design and in some cases can make significant adjustments to the aerodynamic layout of the vehicle. This is because as a result of aerodynamic heating the temperature of the most thermally stressed elements of the structure can exceed the maximum allowable level and lead to the destruction of the structure. That is, the heating would become catastrophic. Therefore, when creating a descent vehicle it is necessary to determine in advance the parameters of heat and mass transfer on its surface, because in this case already at the design stage it will be possible to optimize its geometric, trajectory, weight, and other characteristics, which largely depend on the parameters of necessary thermal protection of the airframe.

For aircraft-type vehicles, it is especially important to determine the thermal conditions of such most heat-stressed areas of the vehicle surface as the fuselage nose and the leading edges of the wings. The maximum temperatures of the outer and inner surfaces of the applied thermal protection coating must not exceed the permissible values. Thus, the thickness of the thermal protection coating depends on the geometry of the apparatus and the trajectory of its re-entry into the Earth's atmosphere.

Since the effective experimental study of high-altitude high-speed viscous gas flows under

*Corresponding author, Ph.D., E-mail: gfon2@yandex.ru

^aPh.D., E-mail: bagarib@yandex.ru

ground conditions is severely limited, and conducting flight experiments is economically expensive and often simply impossible, the need for reliable methods of mathematical modeling of the thermogasodynamics and heat and mass exchange processes is particularly acute in the development of a descent vehicle (Formalev and Kolesnik 2007, Formalev and Kolesnik 2019a, Formalev *et al.* 2009, Formalev *et al.* 2019d, Formalev *et al.* 2020c, Formalev *et al.* 2022, Hein *et al.* 2020). Solving this problem using theoretical approaches is quite difficult since in the high-speed flow near the surface of the apparatus, atomic-molecular high-temperature physical and chemical processes, including relaxation of the internal degrees of freedom of particles, multicomponent diffusion, dissociation, recombination, and ionization in nonequilibrium conditions are fully manifested (Astapov *et al.* 2019, Astapov and Pogodin 2021, Bulychev 2019a, Bulychev 2019b, Bulychev 2019c, Bulychev 2021d, Bulychev 2021e, Bulychev 2022f, Bulychev 2022g, Bulychev 2022h, Bulychev 2022i, Bulychev and Burova 2022, Bulychev and Ivanov 2019a, Bulychev and Ivanov 2019b, Bulychev and Ivanov 2019c, Bulychev and Kolesnik 2022, Bulychev and Rabinskiy 2019a, Bulychev and Rabinskiy 2019b, Burova 2021, Butusova 2020a, Butusova 2020b, Butusova 2020c, Butusova 2020d, Formalev and Kolesnik 2019b, Formalev *et al.* 2019a, Formalev, *et al.* 2019b, Formalev *et al.* 2019c, Formalev *et al.* 2019e, Formalev *et al.* 2020a, Formalev *et al.* 2020b, Goncharenko *et al.* 2022, Ioni 2020a, Ioni 2020b, Ioni 2020c, Ioni and Butusova 2021a, Ioni and Butusova 2021b, Kalugina and Ryapukhin 2021, Kaptakov 2020a, Kaptakov 2020b, Kaptakov 2020c, Kaptakov 2021, Kaptakov *et al.* 2021, Kolesnik 2021a, Kolesnik 2021b, Kolesnik and Bulychev 2020, Kolesnik *et al.* 2019, Kurchatov *et al.* 2019a, Kurchatov, *et al.* 2019b, Lifanov *et al.* 2019, Lifanov *et al.* 2020, Perchenok *et al.* 2021a, Perchenok, *et al.* 2021b, Pogodin *et al.* 2019, Pogodin *et al.* 2020, Rabinskiy and Sitnikov 2018, Radaev 2021a, Radaev 2021b, Radaev 2021c, Sun *et al.* 2020, Tarasova 2020a, Tarasova 2020b, Tarasova 2020c). This set of physical phenomena manifests itself, in macroscopic form, as a wide range of changes in the defining similarity criteria: Mach, Reynolds, Knudsen, Damkeller, Schmidt, Lewis, etc.

In the present work, we performed a numerical simulation of the heat-exchange processes of the most heat-stressed surface areas of a promising small-size winged re-entry vehicle with a mass of 9 t, the layout of which was developed at TsAGI (Bobylev *et al.* 1971). For this purpose, a mathematical model based on solving discrete analogs of the equations of continuum mechanics was used.

2. Task statement

The descent vehicle of TsAGI was chosen as the object of the study (Bobylev *et al.* 1971). This apparatus (Fig. 1) is designed as a “no-tail” with a low-lying double sweep wing.

The apparatus had the following geometrical parameters: length-10.2 m, wingspan-10.3 m, fuselage nose radius $R_0=0.451$ m, a radius of the wing leading edge in the terminal section $R_0=0.078$ m, wingtip angle $\chi_1 = 77^\circ$, wing sweep angle $\chi_2 = 50^\circ$.

For the layout of the small vehicle described above, TsAGI specialists carried out a series of calculations (Bobylev *et al.* 1971), the purpose of which was to find the optimal trajectory that achieves the maximum lateral range for a given limitation of the maximum temperature on the surface of the vehicle. For this purpose, a technique based on the well-known Fay-Riddell relation for equilibrium flow was used (Fay and Riddell 1958).

For those sections of the trajectory where the maximum thermal load was detected, the authors

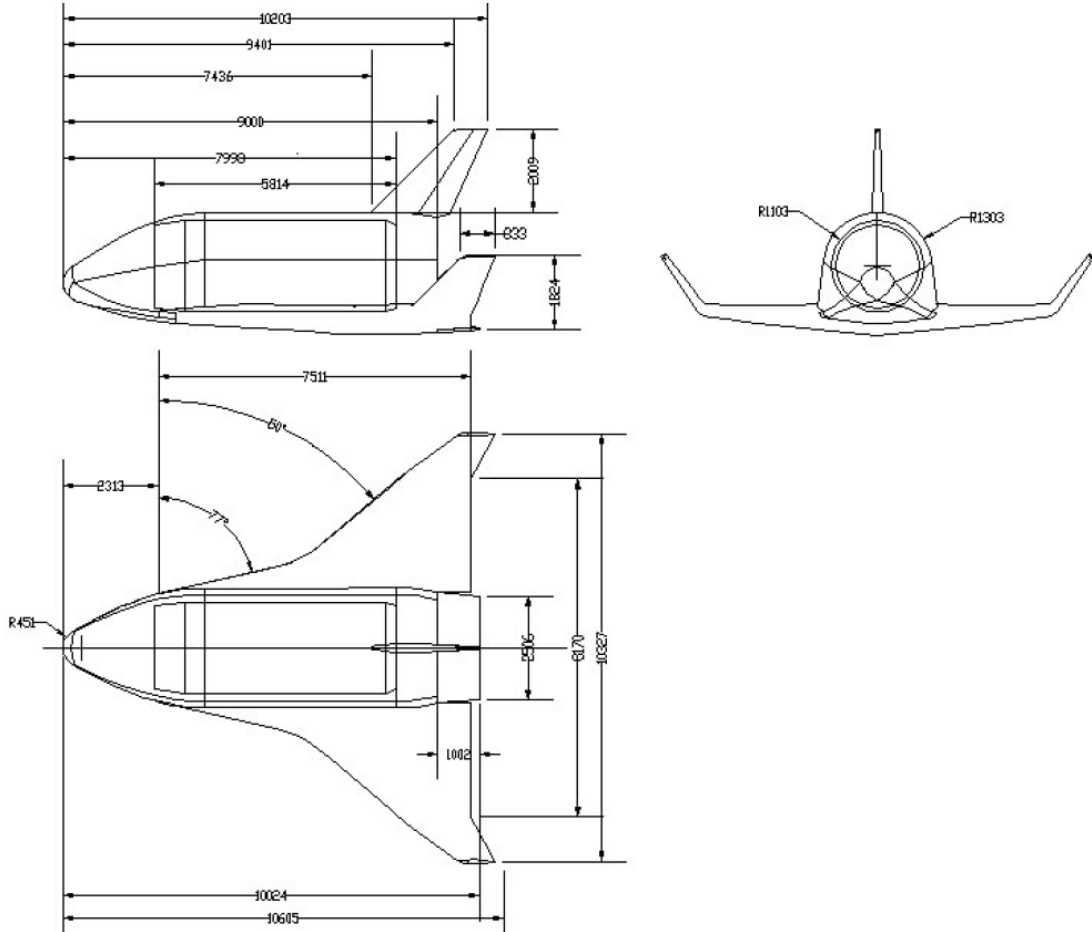


Fig. 1 Exterior view of the TsAGI small-size reentry winged vehicle (Bobylev *et al.* 1971)

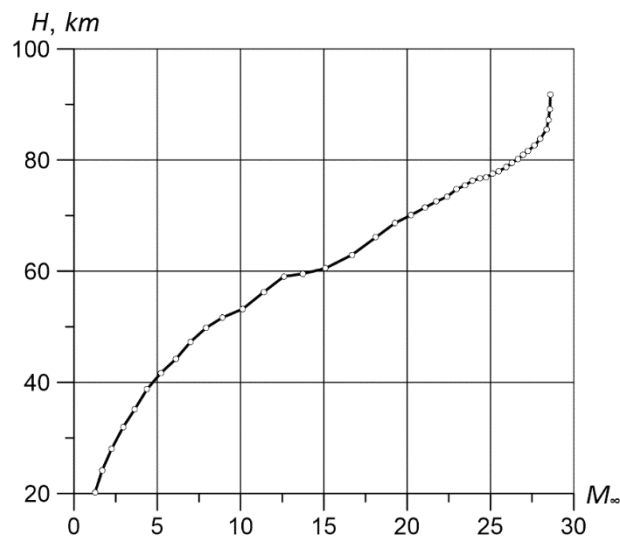


Fig. 2 The trajectory of the descent of the vehicle in the range of heights from 90 km to 20 km

Table 1 Parameters of the incoming flow

Point of trajectory	Altitude H , m	Mach number M_∞	Static pressure p_∞ , Pa	Static temperature T_∞ , K
1	83150	27.80	0.6160	192.5
2	80425	26.75	0.9804	197.8
3	77774	25.33	1.523	203.0
4	73330	22.34	3.114	211.7
5	62675	16.51	15.19	239.7

performed a series of calculations of the two-dimensional nonequilibrium flow around the heat-stressed elements of the apparatus structure using a mathematical model of the viscous boundary layer (Dorrance 2017, Kovalev 2002). These calculations were performed for the case of zero surface catalytic activity.

Fig. 2 shows the extreme heat stress trajectory of the spacecraft's entry into dense layers of the atmosphere (Vaganov *et al.* 2009).

In this study, a series of calculations were performed for five points of the trajectory of descent, located in the region of maximum aerodynamic heating, to compare them with the calculated data of (Bobylev *et al.* 1971). The parameters of the incoming flow for these five points of the trajectory are presented in Table 1.

Since the actual flow parameters realized in front of the leading edge of the wings after passing through the leading shock wave are unknown, it was assumed that the wings, as well as the nose of the fuselage, are flowed by the undisturbed flow. That is, in this formulation, as well as in (Bobylev *et al.* 1971), the braking of the flow due to passage through the head shock wave was not taken into account. The calculations also did not take into account the possible interference of the head shock wave with the shock wave in front of the wing.

Two limiting cases are considered in the study:

- the absolute catalytic activity of the surface of the descent vehicle: $k_w \rightarrow \infty$.
- zero catalytic activity on the surface of the descent vehicle: $k_w \rightarrow 0$.

3. Properties of chemical components

Air was considered as a mixture of 11 components: N_2 , O_2 , NO , N , O , NO^+ , N_2^+ , O_2^+ , N^+ , O^+ , e.

The density of the mixture was calculated as a function of pressure and temperature as follows. The density of the mixture as a function of pressure and temperature was calculated using the ideal gas formula

$$\rho_{cm} = \frac{P_{st}}{R_\mu T \sum_i \frac{C_i}{M_i}}, \quad (1)$$

where P_{st} -local static pressure; $R_\mu = 8,314 \text{ J}/(\text{K} \cdot \text{mol})$ -universal gas constant; T -local static temperature; C_i -mass concentration of the i -th component; M_i -a molar mass of the i -th component.

The specific isobaric heat capacity $c_{p,i}$ of each i -th component was given by the piecewise linear law as a function of temperature (McBride *et al.* 2002). The average specific heat capacity

of the gas mixture was calculated using the ratio

$$c_{p,cm} = \sum_{i=1}^n C_i \cdot c_{p,i} \quad (2)$$

The thermal conductivity coefficient λ_i of each i -th component was calculated using the relation from the kinetic theory of gases (McBride *et al.* 2002) by the formula

$$\lambda_i = \frac{15}{4} \frac{R_\mu}{M_i} \cdot \mu_i \left[\frac{4}{15} \frac{c_{p,i} \cdot M_i}{R_\mu} + \frac{1}{3} \right], \quad (3)$$

where μ_i -dynamic viscosity of the i -th component, function $\mu_i(T)$.

The effective thermal conductivity of the gas mixture was calculated by the formula:

$$\lambda_{cm} = \sum_{i=1}^n C_i \cdot \lambda_i \quad (4)$$

The dynamic viscosity of each component was calculated as a function of static temperature according to the well-known Blottner correlation (Millat *et al.* 1996), and then the dynamic viscosity of the gas mixture was calculated

$$\mu_{cm} = \sum_{i=1}^n C_i \mu_i \quad (5)$$

The molar masses of all components, entropy, and enthalpy values under normal conditions ($P = 101325$ Pa, $T = 298.15$ K) are taken from (Vaganov *et al.* 2009).

4. Chemical kinetics

Taking into account the characteristic timing of chemical processes, the model of nonequilibrium chemistry, consisting of 11 nonequilibrium chemical reactions of dissociation,

Table 2 Parameters of chemical reactions

Number of reaction	Chemical reaction equation	$A_{f,r}$, $\text{m}^3/(\text{kmol} \cdot \text{s})$	$\beta_{f,r}$	$E_{f,r}$, J/ kmol
1	$\text{O}_2 + \text{M} \leftrightarrow 2\text{O} + \text{M}$	2.0e+18	-1.5	4.9471e+08
2	$\text{N}_2 + \text{M} \leftrightarrow 2\text{N} + \text{M}$	7.0e+18	-1.6	9.4120e+08
3	$\text{NO} + \text{M} \leftrightarrow \text{N} + \text{O} + \text{M}$	5.0e+12	0.0	6.2774e+08
4	$\text{N}_2 + \text{O} \leftrightarrow \text{NO} + \text{N}$	6.4e+14	-1.0	3.1928e+08
5	$\text{NO} + \text{O} \leftrightarrow \text{O}_2 + \text{N}$	8.4e+09	0.0	1.6172e+08
6	$\text{N}_2 + \text{e} \leftrightarrow 2\text{N} + \text{e}$	3.0e+21	-1.6	9.4120e+08
7	$\text{N} + \text{e} \leftrightarrow \text{N}^+ + 2\text{e}$	2.5e+31	-3.82	1.4018e+09
8	$\text{O} + \text{e} \leftrightarrow \text{O}^+ + 2\text{e}$	3.9e+30	-3.78	1.3178e+09
9	$\text{N} + \text{O} \leftrightarrow \text{NO}^+ + \text{e}$	5.3e+09	0.0	2.6523e+08
10	$2\text{N} \leftrightarrow \text{N}_2^+ + \text{e}$	2.0e+10	0.0	5.6123e+08
11	$2\text{O} \leftrightarrow \text{O}_2^+ + \text{e}$	1.1e+10	0.0	6.7015e+08

recombination, and ionization, three of which are realized with the participation of third bodies (M) (Table 2), was used in modeling. The empirical coefficients of the kinetics of chemical reactions were taken from (Blottner *et al.* 1971).

For each component of the gas mixture, a separate mass transfer equation was solved in the form

$$\frac{\partial}{\partial t}(\rho_i C_i) + \nabla \cdot (\rho_i \mathbf{u} C_i) = -\nabla \cdot \mathbf{g}_i + \omega_i, \quad (6)$$

where \mathbf{g}_i -diffusion flux of the i -th component; and ω_i -the rate of formation of the i -th component in chemical reactions, which was calculated by the formula

$$\omega_i = M_{w,i} \sum_{r=1}^{N_R} R_{i,r}, \quad (7)$$

where $M_{w,i}$ -a molar mass of the i -th component; N_R -the number of chemical reactions involved in the process and the calculation; $\hat{R}_{i,r}$ - is the molar rate of formation (decay) of the i -th component in reaction r , calculated using the chemical kinetics equation for the rate of formation of the i -th component during a nonequilibrium chemical reaction. The rate $\hat{R}_{i,r}$ in the nonequilibrium chemical reaction r was represented as

$$R_{i,r} = \Gamma (v''_{i,r} - v'_{i,r}) \left(k_{f,r} \prod_{j=1}^N [X_{j,r}]^{\eta'_{j,r}} - k_{b,r} \prod_{j=1}^N [X_{j,r}]^{v''_{j,r}} \right), \quad (8)$$

where $X_{j,r}$ -molar concentration of component j in reaction r (Kmol/m³); $\eta'_{j,r}$ -degree index for reagent j in the reaction r ; $v'_{j,r}$ -the stoichiometric coefficient for reagent j in the reaction r ; $v''_{j,r}$ -the exponent for product j in reaction r (always equal to the stoichiometric coefficient of the reaction product); Γ -coefficient taking into account the effect of third bodies on the reaction rate; $k_{f,r}$ -rate constant of direct reaction; $k_{b,r}$ -rate constant of the reverse reaction.

The rate constant of each direct reaction r was calculated using the Arrhenius expression (McBride *et al.* 2002)

$$k_{f,r} = A_{f,r} T^{\beta_{f,r}} e^{-E_{f,r}/R_u T}, \quad (9)$$

where $A_{f,r}$ -pre-exponential factor; $\beta_{f,r}$ -temperature index; $E_{f,r}$ -reaction activation energy.

The rate constant of each reverse reaction $k_{b,r}$ in Eq. (8) was calculated through the Gibbs free energy change (Landau and Lifshitz 1980).

The efficiencies of each chemical component as the third body (parameter Γ in Eq. (8)), were specified according to (Scalabrin 2007) and presented in Table 3.

5. Calculation grid construction peculiarities

The problem of flow around the surfaces of the fuselage nose and the leading edge of the wing of the investigated apparatus was solved in the three-dimensional formulation.

To save computational resources, the flow around only one-half of the fuselage nose was simulated. In this case, the symmetry boundary condition was set on the OXY plane, which is

Table 3 The efficiency of third bodies

Number of reaction	N ₂	O ₂	NO	N	O	NO+	N ₂ +	O ₂ +	N+	O+	e
1	1	1	1	5	5	1	1	1	5	5	0
2	1	1	1	4,286	4,286	1	1	1	4.286	4.286	0
3	1	1	1	22	22	1	1	1	22	22	0

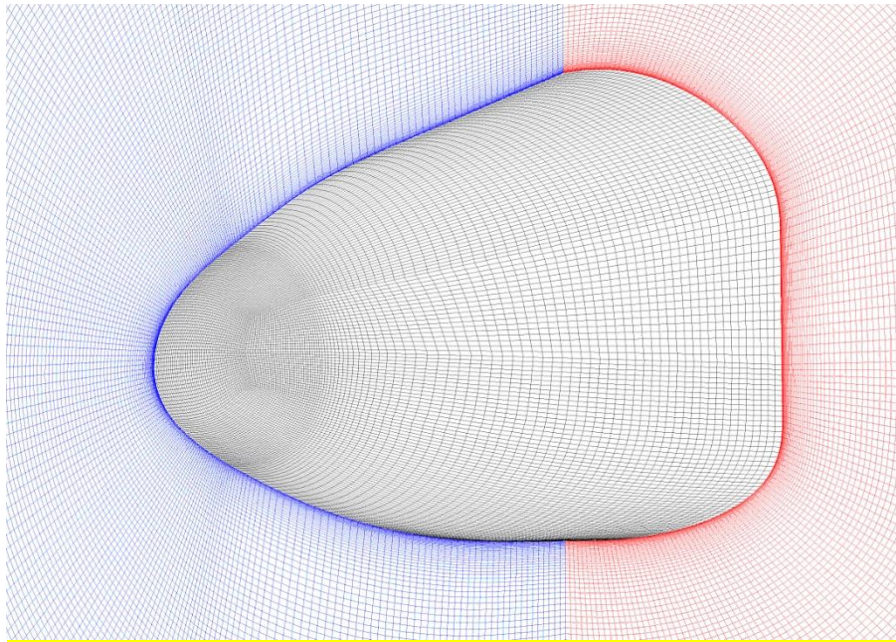


Fig. 3 Calculation grid at the nose of the fuselage

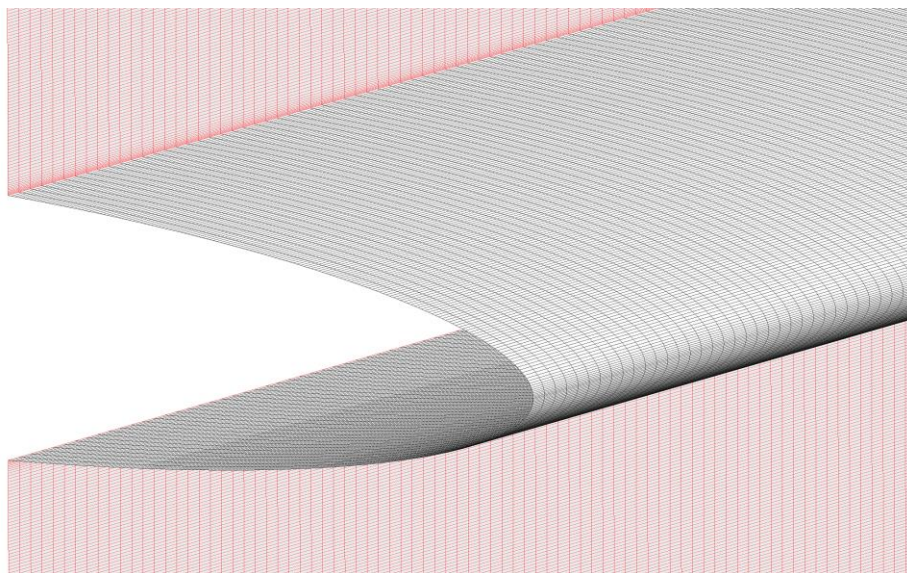


Fig. 4 Calculation grid at the leading edge of the wing (the entrance boundary and the symmetry plane are hidden)

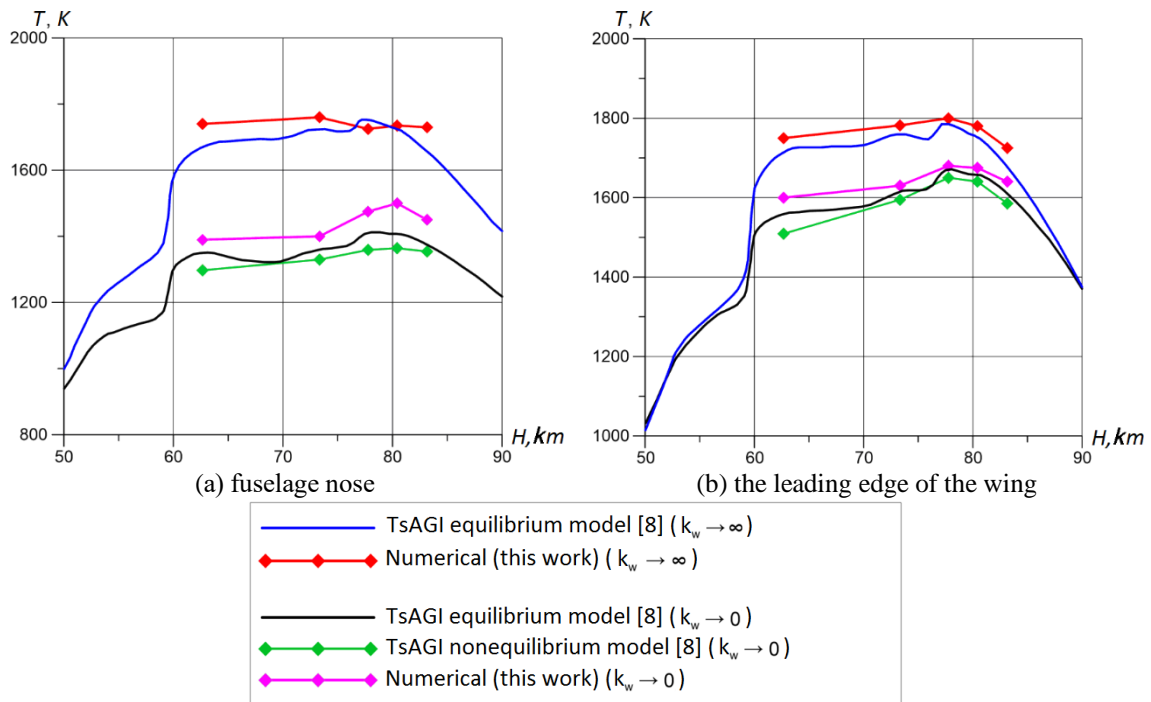


Fig. 5 Variation of the surface temperature of the fuselage nose and the leading edge of the aircraft along the flight trajectory at heights of 90÷50 km

quite acceptable for the glide angle $\beta = 0$. The computational grid for the fuselage nose of 6.6 million cells is shown in Fig. 3, and the grid for the leading edge of the wing of 4.7 million cells is shown in Fig. 4.

6. Calculation results

Fig. 5 shows the temperature dependences of the surface of the fuselage nose and the leading edge of the wing during the flight of the aircraft in the atmosphere along the descent trajectory for the case of absolute catalytic surface activity ($k_w \rightarrow \infty$) and the case of zero catalytic surface activity ($k_w \rightarrow 0$). The results obtained for the surface with $k_w \rightarrow \infty$ were compared with TsAGI calculations (Bobylev *et al.* 1971) performed using the well-known Fay-Riddell relation (equilibrium model).

For the surface with $k_w \rightarrow 0$, the results obtained were compared with calculations by TsAGI (Bobylev *et al.* 1971) carried out both by the Fay-Riddell formula and by a nonequilibrium mathematical model based on the solution of the full system of viscous boundary layer equations.

The data presented in Fig. 5 show that the catalytic activity of the surface has a strong influence on the temperature levels obtained in the calculations. The temperature of the absolutely catalytically active surface is much higher than the temperature of the surface with zero catalytic activity, especially at the descent altitudes of the apparatus from 90 km to 60 km. This can be explained by the fact that at flight altitudes higher than 60 km, a mostly “frozen” boundary layer

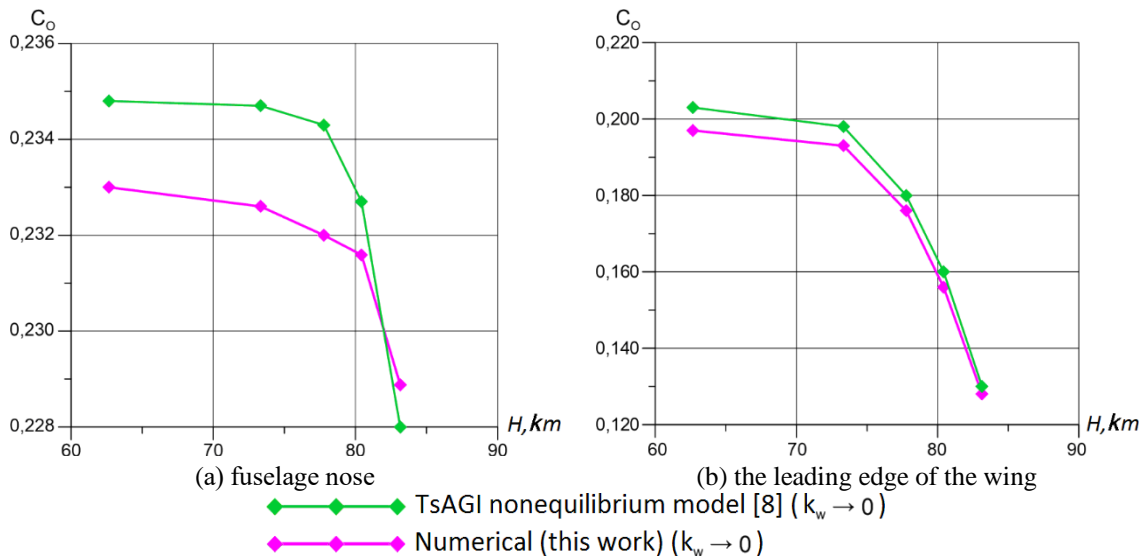


Fig. 6 The concentration of atomic oxygen on the surface of the fuselage nose and wing leading edge

and a partially nonequilibrium boundary layer are realized on the surface of the apparatus. It also follows from the data presented in Figs. 5 and 6 that the results obtained are in satisfactory agreement with the results of calculations using the Fay-Riddell ratio (Bobylev *et al.* 1971) (the maximum deviation does not exceed 7%). At the same time, in some parts of the trajectory, both for the fuselage nose and the leading edge of the wing, the obtained temperature was slightly higher than the data of (Bobylev *et al.* 1971). The reason for this discrepancy is because the Fay-Riddell relation was obtained for an equilibrium chemically active boundary layer and does not take into account the influence of chemical non-equilibrium reactions in the boundary layer on the temperature level of the aircraft surface.

The discrepancy between the data of the present work and the data of calculations using the nonequilibrium mathematical model of TsAGI is obviously due to the difference in the number of nonequilibrium chemical reactions considered. It is known that different formulations of the mechanisms of chemical kinetics can lead to ambiguous results in terms of the apparatus' surface temperature. For example, it was shown in (Landau and Lifshitz 1980) that consideration of chemical nonequilibrium leads to a decrease in the temperature on the surface of the vehicle during flight at an altitude of 22 km in the Mach number range of 6.3÷18.5 compared to the calculation by the Fay-Riddell formula. However, the same work shows that when flying at an altitude of 37 km at a speed corresponding to the Mach number $M_\infty = 17,6$, taking into account the chemical non-equilibrium reactions, on the contrary, leads to an overestimation of the surface temperature of the vehicle.

Nevertheless, it should be noted that the results of calculations of the apparatus surface temperature using mathematical models of different authors have a qualitative correspondence. The quantitative discrepancies do not exceed 10%.

Fig. 6 shows the distribution of atomic oxygen concentrations on the surface of the fuselage nose and the surface of the wing leading edge in the end section. The obtained results are compared with the data of (Scalabrin 2007) for the case of zero surface catalytic activity.

Fig. 6 shows that the obtained results are in satisfactory agreement with the data of (Bobylev *et*

al. 1971), but the concentrations of atomic oxygen at the nose of the fuselage and the leading edge of the wing are somewhat underestimated compared to the TsAGI calculations. The reason for these discrepancies is probably the difference in the rate of chemical reactions occurring in the compressed layer. The reaction rate is known to be determined by the values of the constants in the Arrhenius expression. The fact that the concentrations of atomic oxygen at the fuselage nose and the leading edge of the wing are lower than the concentrations obtained in (Bobylev *et al.* 1971) partially explains the observed overestimation of the surface temperature. Since the dissociation reactions are endothermic, the understated values of atomic oxygen concentrations indicate that the dissociation reactions of oxygen molecules in the boundary layer proceed less intensely than in the calculations of (Bobylev *et al.* 1971) and, therefore, less thermal energy is spent on their realization.

7. Conclusions

A study of heat and mass transfer processes on the most heat-stressed elements of the structure of a small-size winged re-entry vehicle: the nose of the fuselage and the leading edges of the wings was carried out.

It is found that the obtained results are in satisfactory agreement with the calculations according to the Fay-Riddell formula and by solving the equations of the viscous boundary layer.

The dependence of heat fluxes to the surface of the aircraft on its geometric parameters and the catalytic activity of the surface is revealed.

References

- Astapov, A.N. and Pogodin, V.A. (2021), "Change in the integral pore size in CCCM during low-temperature oxidation", *Russian Metallurgy (Metally)*, **2021**(12), 1529-1533. <https://doi.org/10.1134/S0036029521120041>.
- Astapov, A.N., Lifanov, I.P. and Prokofiev, M.V. (2019), "High-temperature interaction in the ZrSi₂-ZrSiO₄ system and its mechanism", *Russian Metallurgy (Metally)*, **6**, 640-646. <https://doi.org/10.1134/S0036029519060065>.
- Blottner, F.G., Johnson, M. and Ellis, M. (1971), *Chemically Reacting Viscous Flow Program for Multi-Component Gas Mixtures*, Sandia Laboratories, Albuquerque, New Mexico, US.
- Bobylev, A.V., Vaganov, A.V., Dmitriev, V.G.E., Zadonsky, S.M., Kireev, A.Y., Skuratov, A.S., ... & Yaroshevsky, V.A. (2010), "Development of aeroshape and investigation of small-sized winged re-entry vehicle aerothermodynamic characteristics", *TsAGI Sci. J.*, **40**, 279-298. <https://doi.org/10.1615/TsAGISciJ.v40.i3.10>.
- Bulychev, N.A. (2019a), "On the hydrogen production during the discharge in a two-phase vapor-liquid flow", *Bull. Lebedev Phys. Inst.*, **46**(7), 219-221. <https://doi.org/10.3103/S1068335619070029>.
- Bulychev, N.A. (2019b), "Hydrogen production in acousto-plasma discharge in a liquid-phase medium flow", *Int. J. Hydrogen Energy*, **44**(57), 29899-29902. <https://doi.org/10.1016/j.ijhydene.2019.09.160>.
- Bulychev, N.A. (2019c), "Experimental studies on hydrogen production in plasma discharge in a liquid-phase medium flow", *Int. J. Hydrogen Energy*, **44**(57), 29933-29936. <https://doi.org/10.1016/j.ijhydene.2019.09.177>.
- Bulychev, N.A. (2021d), "Obtaining of nanosized materials in plasma discharges and ultrasonic cavitation", *High Temperat.*, **59**(4), 600-633.
- Bulychev, N.A. (2021e), "Preparation of stable suspensions of ZnO nanoparticles with ultrasonically

- assisted low-temperature plasma”, *Nanosci. Technol.*, **12**(3), 91-97. <https://doi.org/10.1615/NanoSciTechnolIntJ.2021038033>.
- Bulychev, N.A. (2022f), “Acoustoplasma synthesis of silver nanoparticles with antibacterial properties”, *Biophys. J.*, **121**(3), 427a. <https://doi.org/10.1016/j.bpj.2021.11.649>.
- Bulychev, N.A. (2022g), “Study of interaction of surface-active polymers with ZnO nanoparticles synthesized in ultrasonically assisted plasma discharge”, *Nanosci. Technol.*, **13**(1), 55-65. <https://doi.org/10.1615/NanoSciTechnolIntJ.2021038100>.
- Bulychev, N.A. (2022h), “Obtaining of gaseous hydrogen and silver nanoparticles by decomposition of hydrocarbons in ultrasonically stimulated low-temperature plasma”, *Int. J. Hydrogen Energy*, **47**(50), 21323-21328. <https://doi.org/10.1016/j.ijhydene.2022.04.288>.
- Bulychev, N.A. (2022i), “Synthesis of gaseous hydrogen and nanoparticles of silicon and silica by pyrolysis of tetraethoxysilane in an electric discharge under the ultrasonic action”, *Int. J. Hydrogen Energy*, **47**(84), 35581-35587. <https://doi.org/10.1016/j.ijhydene.2022.08.163>.
- Bulychev, N.A. and Burova, A.Y. (2022), “Unerroric of control of mutual compliance of the efficiency of hydrogen engines of unmanned vehicles in the conditions of mass production”, *Int. J. Hydrogen Energy*, **47**(63), 26789-26797. <https://doi.org/10.1016/j.ijhydene.2022.06.078>.
- Bulychev, N.A. and Ivanov, A.V. (2019a), “Effect of vibration on structure and properties of polymeric membranes”, *Int. J. Nanotechnol.*, **16**(6/7/8/9/10), 334-343. <https://doi.org/10.1504/IJNT.2019.106609>.
- Bulychev, N.A. and Ivanov, A.V. (2019b), “Nanostructure of organic-inorganic composite materials based on polymer hydrogels”, *Int. J. Nanotechnol.*, **16**(6/7/8/9/10), 344-355. <https://doi.org/10.1504/IJNT.2019.106610>.
- Bulychev, N.A. and Ivanov, A.V. (2019c), “Study of nanostructure of polymer adsorption layers on the particles surface of titanium dioxide”, *Int. J. Nanotechnol.*, **16**(6/7/8/9/10), 356-365. <https://doi.org/10.1504/IJNT.2019.106611>.
- Bulychev, N.A. and Kolesnik, S.A. (2022), “Reinforcement of polymer composite materials by titanium dioxide nanoparticles synthesized in plasma discharge under ultrasonic cavitation”, *IOP Conf. Proc.*, **2231**, 012012.
- Bulychev, N.A. and Rabinskiy, L.N. (2019a), “Ceramic nanostructures obtained by acoustoplasma technique”, *Nanosci. Technol.*, **10**(3), 279-286. <https://doi.org/10.1615/NanoSciTechnolIntJ.2019031161>.
- Bulychev, N.A. and Rabinskiy, L.N. (2019b), “Surface modification of titanium dioxide nanoparticles with acrylic acid/isobutylene copolymer under ultrasonic treatment”, *Periodico Tche Quimica*, **16**(32), 338-344.
- Burova, A.Y. (2021), “Concept of multistage discrete fourier transform without performing multiplications”, *J. Phys.: Conf. Ser.*, **1889**(2), 022003.
- Butusova, O.A. (2020a), “Adsorption behaviour of ethylhydroxyethyl cellulose on the surface of microparticles of titanium and ferrous oxides”, *Int. J. Pharmaceut. Res.*, **12**(2), 1156-1159.
- Butusova, O.A. (2020b), “Stabilization of carbon microparticles by high-molecular surfactants”, *Int. J. Pharmaceut. Res.*, **12**(2), 1147-1151.
- Butusova, O.A. (2020c), “Surface modification of titanium dioxide microparticles under ultrasonic treatment”, *Int. J. Pharmaceut. Res.*, **12**(4), 2292-2296.
- Butusova, O.A. (2020d), “Vinyl ether copolymers as stabilizers of carbon black suspensions”, *Int. J. Pharmaceut. Res.*, **12**(2), 1152-1155.
- Dorrance, W.H. (2017), *Viscous Hypersonic Flow. Theory of Reacting Hypersonic Boundary Layers*, Dover Publications, Inc., New York, US.
- Fay, J. and Riddell, F. (1958), “Theory of stagnation point heat transfer in dissociated air”, *J. Aeronaut. Sci.*, **25**(2), 73-85. <https://doi.org/10.2514/8.7517>.
- Formalev, V.F. and Kolesnik, S.A. (2007), “Conjugate heat transfer between wall gasdynamic flows and anisotropic bodies”, *High Temp.*, **45**, 76-84. <https://doi.org/10.1134/S0018151X07010105>.
- Formalev, V.F. and Kolesnik, S.A. (2019a), *Mathematical Modeling of Coupled Heat Transfer Between Viscous Gas-Dynamic Flows and Anisotropic Bodies*, Lenand, Moscow, Russia.
- Formalev, V.F. and Kolesnik, S.A. (2019b), “On thermal solitons during wave heat transfer in restricted

- areas”, *High Temperat.*, **57**(4), 498-502. <https://doi.org/10.1134/S0018151X19040047>.
- Formalev, V.F., Bulychev, N.A., Kolesnik, S.A. and Kazaryan, M.A. (2019a), “Thermal state of the package of cooled gas-dynamic microlasers”, *Proc. SPIE-Int. Soc. Opt. Eng.*, **11322**, 113221B. <https://doi.org/10.1117/12.2550771>.
- Formalev, V.F., Bulychev, N.A., Kuznetsova, E.L. and Kolesnik, S.A. (2020a), “The thermal state of a packet of cooled microrocket gas-dynamic lasers”, *Tech. Phys. Lett.*, **46**(3), 245-248. <https://doi.org/10.1134/S1063785020030074>.
- Formalev, V.F., Kartashov, E.M. and Kolesnik, S.A. (2019b), “Simulation of nonequilibrium heat transfer in an anisotropic semispace under the action of a point heat source”, *J. Eng. Phys. Thermophys.*, **92**(6), 1537-1547. <https://doi.org/10.1007/s10891-019-02074-7>.
- Formalev, V.F., Kartashov, E.M. and Kolesnik, S.A. (2020b), “On the dynamics of motion and reflection of temperature solitons in wave heat transfer in limited regions”, *J. Eng. Phys. Thermophys.*, **93**(1), 10-15. <https://doi.org/10.1007/s10891-020-02085-9>.
- Formalev, V.F., Kolesnik, S.A. and Garibyan, B.A. (2020c), “Analytical solution of the problem of conjugate heat transfer between a gasdynamic boundary layer and anisotropic strip”, *Herald Bauman Moscow State Tech. Univ., Ser. Nat. Sci.*, **5**(92), 44-59.
- Formalev, V.F., Kolesnik, S.A. and Garibyan, B.A. (2022), “Mathematical modeling of heat and mass transfer during aerodynamic heating of the nose parts of hypersonic aircraft”, *Herald Bauman Moscow State Tech. Univ., Ser. Nat. Sci.*, **1**(100), 107-121.
- Formalev, V.F., Kolesnik, S.A. and Kuznetsova, E.L. (2009), “The effect of longitudinal nonisothermality on conjugate heat transfer between wall gasdynamic flows and blunt anisotropic bodies”, *High Temp.*, **47**, 228. <https://doi.org/10.1134/S0018151X09020138>.
- Formalev, V.F., Kolesnik, S.A. and Kuznetsova, E.L. (2019c), “Approximate analytical solution of the problem of conjugate heat transfer between the boundary layer and the anisotropic strip”, *Periodico Tche Quimica*, **16**(32), 572-582.
- Formalev, V.F., Kolesnik, S.A. and Kuznetsova, E.L. (2019d), “Effect of components of the thermal conductivity tensor of heat-protection material on the value of heat fluxes from the Gasdynamic boundary layer”, *High Temp.*, **57**, 66-71. <https://doi.org/10.1134/S0018151X19010085>.
- Formalev, V.F., Kolesnik, S.A. and Kuznetsova, E.L. (2019e), “Mathematical modeling of a new method of thermal protection based on the injection of special coolants”, *Periodico Tche Quimica*, **16**(32), 598-607.
- Goncharenko, V., Mikhaylov, Y. and Kartushina, N. (2022), “Pattern recognition techniques for classifying aeroballistic flying vehicle paths”, *Neur. Comput. Appl.*, **34**(5), 4033-4045. <https://doi.org/10.1007/s00521-021-06662-8>.
- Hein, T.Z., Garibyan, B.A., Vakhneev, S.N., Tushavina, O.V. and Formalev, V.F. (2020), “Analytical study of joint heat transfer between a gas-dynamic boundary layer and an anisotropic strip”, *INCAS Bull.*, **12**, 233-243.
- Ioni, Y.V. (2020a), “Effect of ultrasonic treatment on properties of aqueous dispersions of inorganic and organic particles in presence of water-soluble polymers”, *Int. J. Pharmaceut. Res.*, **12**(4), 3440-3442.
- Ioni, Y.V. (2020b), “Nanoparticles of noble metals on the surface of graphene flakes”, *Periodico Tche Quimica*, **17**(36), 1199-1211.
- Ioni, Y.V. (2020c), “Synthesis of metal oxide nanoparticles and formation of nanostructured layers on surfaces under ultrasonic vibrations”, *Int. J. Pharmaceut. Res.*, **12**(4), 3432-3435.
- Ioni, Y.V. and Butusova, O.A. (2021a), “Preparation of polymer composite material with Fe₂O₃ nanoparticles synthesized with low-temperature plasma under ultrasonic action”, *AIP Conf. Proc.*, **2402**, 020035. <https://doi.org/10.1063/5.0071390>.
- Ioni, Y.V. and Butusova, O.A. (2021b), “Synthesis of Al₂O₃ nanoparticles for their subsequent use as fillers of polymer composite materials”, *AIP Conf. Proc.*, **2402**, 020036. <https://doi.org/10.1063/5.0071387>.
- Kalugina, G.A. and Ryapukhin, A.V. (2021), “Impact of the 2020 pandemic on Russian aviation”, *Russian Eng. Res.*, **41**(7), 627-630. <https://doi.org/10.3103/S1068798X21070133>.
- Kaptakov, M.O. (2020a), “Catalytic desulfuration of oil products under ultrasonic treatment”, *Int. J. Pharmaceut. Res.*, **12**(2), 1838-1843.

- Kaptakov, M.O. (2020b), "Effect of ultrasonic treatment on stability of TiO₂ aqueous dispersions in presence of water-soluble polymers", *Int. J. Pharmaceut. Res.*, **12**(2), 1821-1824.
- Kaptakov, M.O. (2020c), "Enhancement of quality of oil products under ultrasonic treatment", *Int. J. Pharmaceut. Res.*, **12**(2), 1851-1855.
- Kaptakov, M.O. (2021), "Synthesis and characterization of polymer composite materials based on polyethylene and CuO nanoparticles", *AIP Conf. Proc.*, **2402**, 020027. <https://doi.org/10.1063/5.0071381>.
- Kaptakov, M.O., Pegachkova, E.A. and Makarenko, A.V. (2021), "Physical and mechanical properties of composites polyethylene-CuO nanoparticles", *AIP Conf. Proc.*, **2402**, 020038. <https://doi.org/10.1063/5.0071378>.
- Kolesnik, S.A. (2021a), "Investigation of mechanical properties of polymer composite material based on polyethylene with Fe₂O₃ nanoparticles", *AIP Conf. Proc.*, **2402**, 020037. <https://doi.org/10.1063/5.0071380>.
- Kolesnik, S.A. (2021b), "Mechanical properties of polyethylene/Al₂O₃ nanoparticles composite material", *AIP Conf. Proc.*, **2402**, 020026. <https://doi.org/10.1063/5.0071384>.
- Kolesnik, S.A. and Bulychev, N.A. (2020), "Numerical analytic method for solving the inverse coefficient problem of heat conduction in anisotropic half-space", *J. Phys.: Conf. Ser.*, **1474**(1), 012024. <https://doi.org/10.1088/1742-6596/1474/1/012024>.
- Kolesnik, S.A., Bulychev, N.A., Rabinskiy, L.N. and Kazaryan, M.A. (2019), "Mathematical modeling and experimental studies of thermal protection of composite materials under high-intensity effects of laser radiation", *Proc. SPIE-Int. Soc. Opt. Eng.*, **11322**, 113221R. <https://doi.org/10.1117/12.2553955>.
- Kovalev, V.L. (2002), *Heterogeneous Catalytic Processes in Aerothermodynamics*, Fizmatlit, Moscow, Russia.
- Kurchatov, I., Bulychev, N., Kolesnik, S. and Muravev, E. (2019b), "Application of the direct matrix analysis method for calculating the parameters of the luminescence spectra of the iron ion in zinc sulfide crystals", *AIP Conf. Proc.*, **2181**, 020015. <https://doi.org/10.1063/1.5135675>.
- Kurchatov, I.S., Bulychev, N.A. and Kolesnik, S.A. (2019a), "Obtaining spectral characteristics of semiconductors of AIBVI type alloyed with iron ions using direct matrix analysis", *Int. J. Recent Technol. Eng.*, **8**(3), 8328-8330.
- Landau, L.D. and Lifshitz, E.M. (1980), *Statistical Physics*, Pergamon Press, Oxford, UK.
- Lifanov, I.P., Astapov, A.N. and Terentjeva, V.S. (2020), "Deposition of heat-resistant coatings based on the ZrSi₂-MoSi₂-ZrB₂ system for protection of non-metallic composite materials in high-speed high-enthalpy gas flows", *J. Phys.: Conf. Ser.*, **1713**(1), 012025. <https://doi.org/10.1088/1742-6596/1713/1/012025>.
- Lifanov, I.P., Yurishcheva, A.A. and Astapov, A.N. (2019), "High-temperature protective coatings on carbon composites", *Russian Eng. Res.*, **39**(9), 804-808. <https://doi.org/10.3103/S1068798X19090132>.
- McBride, B.J., Zehe M.J. and Gordon, S. (2002), *NASA Glenn Coefficients for Calculating Thermodynamic Properties of Individual Species*, National Aeronautics and Space Administration John H. Glenn Research Center at Lewis Field Cleveland, US.
- Millat, J., Dymond, J.H. and Nieto de Castro, C. A. (1996), *Transport Properties of Fluids: Their Correlation, Prediction and Estimation*, Cambridge University Press, Cambridge, UK.
- Perchenok, A.V., Suvorova, E.V., Farmakovskaya, A.A. and Kohlert V. (2021b), "Stabilization of aqueous dispersions of inorganic microparticles under mechanical activation", *WSEAS Trans. Appl. Theor. Mech.*, **16**, 127-133.
- Perchenok, A.V., Suvorova, E.V., Farmakovskaya, A.A. and Kohlert, V. (2021a), "Application of vinyl ether copolymers for surface modification of carbon black", *Int. J. Circuit., Syst. Signal Pr.*, **15**, 1414-1420.
- Pogodin, V.A., Astapov, A.N. and Rabinskiy, L.N. (2020), "CCCM specific surface estimation in process of low-temperature oxidation", *Periodico Tche Quimica*, **17**(34), 793-802.
- Pogodin, V.A., Rabinskii, L.N. and Sitnikov, S.A. (2019), "3D printing of components for the gas-discharge chamber of electric rocket engines", *Russian Eng. Res.*, **39**(9), 797-799. <https://doi.org/10.3103/S1068798X19090156>.

- Rabinskiy, L.N. and Sitnikov, S.A. (2018), "Development of technologies for obtaining composite material based on silicone binder for its further use in space electric rocket engines", *Periodico Tche Quimica*, **15**(1), 390-395.
- Radaev, S. (2021a), "Design calculations of the limiting characteristics of heat pipes for cooling active phased antenna arrays", *WSEAS Trans. Appl. Theor. Mech.*, **16**, 142-149.
- Radaev, S. (2021b), "Mathematical modeling of heat and mass transfer in heat pipes in a one-dimensional formulation when cooling active phased antenna arrays", *Int. J. Mech.*, **15**, 196-203.
- Radaev, S. (2021c), "Numerical and analytical modeling of permanent deformations in panels made of nanomodified carbon fiber reinforced plastic with asymmetric packing", *Int. J. Mech.*, **15**, 172-180.
- Scalabrin, L.C. (2007), *Numerical Simulation of Weakly Ionized Hypersonic Flow over Reentry Capsules*. University of Michigan, Michigan, US.
- Sun, Y., Kolesnik, S.A. and Kuznetsova, E.L. (2020), "Mathematical modeling of coupled heat transfer on cooled gas turbine blades", *INCAS Bull.*, **12**, 193-200.
- Tarasova, A.N. (2020a), "Effect of reagent concentrations on equilibria in water-soluble complexes", *Int. J. Pharmaceut. Res.*, **12**(2), 1169-1172.
- Tarasova, A.N. (2020b), "Effect of vibration on physical properties of polymeric latexes", *Int. J. Pharmaceut. Res.*, **12**(2), 1173-1180.
- Tarasova, A.N. (2020c), "Vibration-based method for mechanochemical coating metallic surfaces", *Int. J. Pharmaceut. Res.*, **12**(2), 1160-1168.
- Vaganov, A.V., Drozdov, S., Kosykh, A.P., Nersesov, G.G., Chelysheva, I.F. and Yumashev, V.L. (2009), "Numerical simulation of aerodynamics of winged reentry space vehicle", *TsAGI Sci. J.*, **40**, 131-149. <https://doi.org/10.1615/TsAGISciJ.v40.i2.10>.